Calorimetric Study of Maghemite Nanoparticles Synthesized by Laser-Induced Pyrolysis

Oscar Bomatí-Miguel,[†,⊥] Lena Mazeina,[†,§] Alexandra Navrotsky,*[,†] and Sabino Veintemillas-Verdaguer[‡]

Peter A. Rock Thermochemistry Laboratory and NEAT ORU, University of California at Davis, One Shields Avenue, Davis, California 95616, and Instituto de Ciencia de Materiales de Madrid, CSIC, C/Sor Juana Inés de la Cruz 3, Campus de Cantoblanco, Madrid 28049, Spain

Received May 1, 2007. Revised Manuscript Received November 21, 2007

The thermodynamic properties of maghemite (γ-Fe_2O_3) nanoparticles with size smaller than 10 nm had not been studied previously because of particle size limitations for samples synthesized by wet chemical methods. Laser-induced pyrolysis is a well-established method of producing maghemite with particle sizes smaller than 10 nm. Maghemite nanoparticles, obtained by this method and having a size range of 2–40 nm, were fully characterized and studied by solution calorimetry. The enthalpy of water adsorption was also measured. The surface enthalpy obtained from calorimetric data for the hydrated maghemite surface is 0.57 ± 0.10 J/m^2 and is in good agreement with previously reported values. The surface enthalpy for the dry, water-free surface is 0.71 ± 0.13 J/m^2 and is reported for the first time. The difference in the surface enthalpy for the dry surface between α- and γ-polymorphs of Fe_2O_3 is similar to that between α- and γ-Al_2O_3. This large difference in surface enthalpy ($\sim$1.2 J/m^2) creates an energy crossover so that fine-grained hematite is metastable relative to fine-grained maghemite at particle size $<$15 nm.

Introduction

Maghemite, γ-Fe_2O_3, nanoparticles are routinely used in applications from refrigeration to biomedicine.[1–5] A fundamental characteristic of ultrafine particles is that a large fraction of atoms is located at or near the surface. The surface energy makes a significant contribution to the total energy, stability, and reactivity of these nanoparticles.[6]

While there have been many investigations of the variations of physical properties of nano-maghemite, there have been comparatively few studies of thermodynamic properties of such nanoparticles. Calorimetric studies of surface thermodynamic properties of maghemite are restricted to bulk and well-crystallized materials[7–12] obtained by wet chemical syntheses. This method does not produce ultrafine particles, and the calorimetric data are limited to samples with surface areas not exceeding $\sim$100 m^2/g. Laser pyrolysis is a well-established method of obtaining maghemite with particle sizes smaller than 10 nm.[13–15]

In this work, we report calorimetric characterization of nano-maghemite with surface areas up to $\sim$200 m^2/g and particle size 2–40 nm that were obtained by laser-induced pyrolysis of iron pentacarbonyl vapor. The nanoparticles were characterized by X-ray diffraction, transmission electron microscopy, surface area analysis, Fourier transform infrared spectroscopy, and Mössbauer spectroscopy. Characterization of the adsorbed water by thermogravimetry, weight loss on ignition, and water adsorption calorimetry was especially important since surfaces of nanoparticles adsorb a significant amount of water, which affects interpretation of the solution calorimetric results.

Experimental Section

Synthesis. All reagent grade chemicals (purity $>$99.9%) were purchased and used without additional purification. Maghemite

* To whom correspondence should be addressed: e-mail anavrotsky@ucdavis.edu.
† University of California at Davis.
‡ CSIC.
§ Current address: Naval Research Laboratory, 4555 Overlook Ave., Washington, DC 20375.
⊥ Current address: Nanoporous Films and Particles Research Group, CiBER-BBN, Nanoscience Institute of Aragon, University of Zaragoza, C/Pedro Cerbuna 12, Zaragoza 50009, Spain.

(1) Tartaj, P.; Morales, M. P.; Veintemillas-Verdaguer, S.; Gonzalez-Carreño, T.; Serna, C. J. *J. Phys. D: Appl. Phys.* **2003**, *36*, R182.
(2) Brigger, I.; Dubernet, C.; Couvreur, P. *Adv. Drug Delivery Rev.* **2002**, *54*, 631.
(3) Morales, M. P.; Bomati-Miguel, O.; Pérez de Alejo, R.; Ruiz-Cabello, J.; Veintemillas-Verdaguer, S.; O'Grady, K. *J. Magn. Magn. Mater.* **2003**, *266*, 102.
(4) Veintemillas-Verdaguer, S.; Morales, M. P.; Bomati-Miguel, O.; Bautista, C.; Zhao, X.; Bonville, P.; Perez de Alejo, R.; Ruiz-Cabello, J.; Santos, M.; Tendillo-Cortijo, F. J.; Ferreiros, J. *J. Phys. D: Appl. Phys.* **2004**, *37*, 2054.
(5) Gupta, A. K.; Gupta, M. *Biomaterials* **2005**, *26*, 3995.
(6) Li, P.; Miser, D. E.; Rabiei, S.; Yadav, R. T.; Hajaligol, M. R. *Appl. Catal., B* **2003**, *43*, 151.
(7) Diakonov, I. I. *Eur. J. Miner.* **1998**, *10*, 17.
(8) Fricke, R.; Zerrweck, W. *Z. Elektrochem. Angew. Phys. Chem.* **1937**, *43*, 52.
(9) Laberty, C.; Navrotsky, A. *Geochim. Cosmochim. Acta* **1998**, *62*, 2905.
(10) Majzlan, J.; Lang, B. E.; Stevens, R.; Navrotsky, A.; Woodfield, B. F.; Boerio-Goates, J. *Am. Mineral.* **2003**, *88*, 846.
(11) Majzlan, J.; Grevel, K. D.; Navrotsky, A. *Am. Mineral.* **2003**, *88*, 855.
(12) Majzlan, J. Thermodynamic of iron and aluminium oxides. Ph.D. Dissertation, University of California at Davis, Davis, CA, 2003.
(13) Veintemillas-Verdaguer, S.; Morales, M. P.; Serna, C. J. *Mater. Lett.* **1998**, *35*, 227.
(14) Veintemillas-Verdaguer, S.; Bomatí-Miguel, O.; Morales, M. P. *Scr. Mater.* **2002**, *47*, 589.
(15) Veintemillas-Verdaguer, S.; Morales, M. P.; Serna, C. J. *Appl. Organomet. Chem.* **2001**, *15*, 365.

10.1021/cm071178o CCC: $40.75
Published on Web 01/01/2008

Table 1. Synthesis Conditions and Characterization Results (Carbon Content, Crystal Size, Particle Size, and BET Surface Area) of Maghemite Nanoparticles

sample, ID	Fe/O_2 molar ratio	BET surface area, m^2/g	XRD crystal size, nm	TEM particle size, nm	carbon content		water content x, in $Fe_2O_3 \cdot xH_2O \cdot yC$, mol
					wt %	y, in $Fe_2O_3 \cdot xH_2O \cdot yC$, mol	
Ah-1	1.00	126.3 ± 1.2	11	8 ± 3	0.7	0.10	0.507 ± 0.006
Ah-2	1.00	143.4 ± 1.2	9	8 ± 2	1.5	0.22	0.52 ± 0.05
Ah-3	0.90	153.7 ± 1.4	8	4 ± 2	1.2	0.17	0.47 ± 0.04
Ah-4	0.55	173.9 ± 1.3	4	3 ± 2	1.6	0.23	0.58 ± 0.06
As-5	0.50	182.5 ± 1.4	4	10 ± 1	1.7	0.25	0.62 ± 0.05
As-6	0.30	187.3 ± 1.1	3	8 ± 2	1.2	0.18	0.93 ± 0.03
As-7	0.27	203.3 ± 1.1	3	4 ± 1	1.6	0.23	0.59 ± 0.08
Ah-8	0.01	214.3 ± 1.2	2	4 ± 1	0.9	0.19	0.77 ± 0.06
B-1		23.4 ± 0.6	43		0.2	0.02	0.11 ± 0.02
B-2		55.2 ± 0.2	30		0.2	0.03	0.21 ± 0.03
C-1		24.1 ± 0.4	>100				0.12 ± 0.01

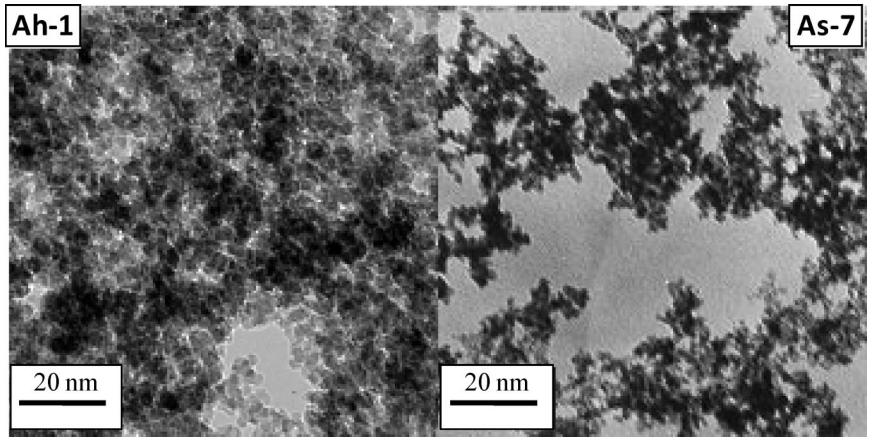

Figure 1. TEM images of maghemite samples obtained by laser-induced pyrolysis: hard oxidation (left, sample Ah-1) and soft oxidation (right, sample As-7).

nanoparticles were obtained by in-situ hard[13,14] and soft[15] laser decomposition of gaseous $Fe(CO)_5$ in air (sample batches Ah and As, respectively; see Table 1). Changing the initial Fe/O_2 ratio in the system controlled the particle size.[14,15] Samples in batch B were synthesized by the oxidation of iron nanoparticles[16] 30 and 14 nm in size by heating them in air at 673 K. The physical properties of the samples are listed in Table 1. Sample C-1 is the coarse-grained sample used in previous investigations.[10–12] The surface area and water content measured in our work for this sample agree with those previously reported.[10,11]

Characterization. X-ray diffraction patterns were collected from 10° to 90° (2θ) with a step size of 0.02° and a dwell time of 1.2 s. The Scintag PAD V diffractometer had a Cu X-ray tube, and a solid-state detector allowed electronic filtering to remove the high background from iron fluorescence. Lattice parameter and crystallite domain size (D_{XRD}) were determined from the X-ray profiles using Rietveld analysis and the Scherrer equation, respectively, using JADE 6.1 software (Materials Data Inc., 2001). Lattice parameters of maghemite agree with the literature values within the experimental errors. All maghemite samples showed pure maghemite, except coarse-grained samples B-1 and B-2 where about 8% hematite was found by the refinement.

Morphology and particle size distribution were analyzed by transmission electron microscopy (TEM) using a JEOL TEM-2000FX microscope operated at 200 keV (see Figure 1). Sizes of ~100 particles were measured. In general, average particle size obtained by TEM agrees well with that calculated from XRD patterns using the Scherrer equation (see Table 1).

Mössbauer spectra were collected using a standard spectrometer with a maximum velocity of 10 mm s^{-1} and a ^{57}Co:Rh source at $T = 5$ K. The isomer shifts are reported with respect to α-Fe, and the spectra are fitted using a standard minimization of the χ^2 procedure. The spectra show the six well-defined peaks of the magnetic hyperfine field of maghemite.

Fourier transform infrared spectroscopy (FTIR) of the iron oxide powders diluted in KBr was done with a Bruker Equinox 55 spectrometer. The FTIR spectra were recorded between 850 and 350 cm^{-1} for the main absorption bands associated with O−Fe vibrational modes.[17]

The specific surface area of the maghemite particles was measured by the multipoint Brunauer–Emmett–Teller (BET) method[18] using a Micromeritics ASAP 2020 gas adsorption apparatus. All samples were prepared for analysis by degassing at 423 K for at least 12 h prior to the measurement.

Carbon content of the samples was determined by ICP-OES elemental analysis (Perkin-Elmer 2400CHN). Residual carbon content was found to be less than 2 wt % (Table 1).

Thermogravimetric and differential thermal analyses (TGA/DTA) were made with a Netzsch 449 thermal analysis system in air from 298 to 1200 K with a heating rate 10 K/min (Figure 2). No weight gain, suggesting negligible ferrous iron content, was observed during the analysis.

Water content was determined from furnace experiments by heating the samples at 1373 K overnight in corundum crucibles

(16) Bomati-Miguel, O.; Tartaj, P.; Morales, M. P.; Bonville, P.; Golla-Schindler, U.; Zhao, X. Q.; Veintemillas-Verdaguer, S. *Small* **2006**, *2*, 1476.

(17) Cornell, R. M.; Schwertmann, U. *The Iron Oxides: Structure, Properties, Reactions, Occurrence and Uses*; VCH: Berlin, 1996.

(18) Brunauer, S.; Emmett, P. H.; Teller, E. *J. Am. Chem. Soc.* **1938**, *60*, 309.

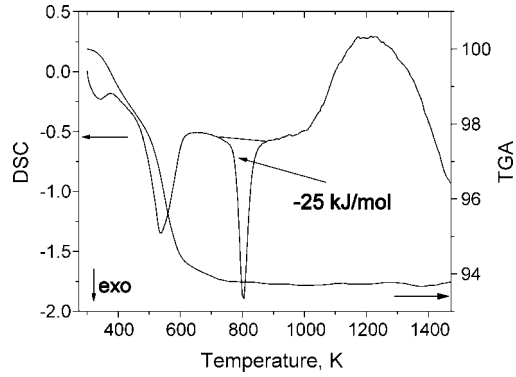

Figure 2. DTA−TGA curves of the sample Ah-8. Two exothermic peaks correspond (1) to carbon oxidation (dominating exothermic process) and partially to water release (endothermic process) and (2) to maghemite transformation to hematite (~800 K).

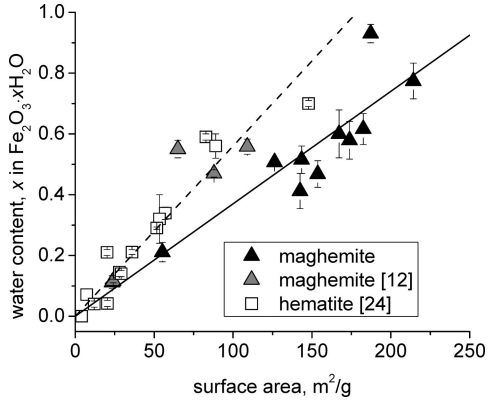

Figure 3. Water content as function of surface area in comparison with literature data[12] and with hematite water content.[24] Straight lines represent linear fits of the hematite and maghemite data.

first heated to the same temperature. The amount of adsorbed water x was calculated from total weight loss for the reaction:

$$\gamma\text{-}Fe_2O_3{\cdot}xH_2O{\cdot}yC + O_2 = \alpha\text{-}Fe_2O_3 + xH_2O + yCO_2 \quad (1)$$

using the formula

$$\frac{m_f}{m_i} = \frac{MW(Fe_2O_3)}{MW(Fe_2O_3) + xMW(H_2O) + yMW(C)} \quad (2)$$

where MW stand for molecular weight, m_f and m_i are final and initial sample weights, respectively, and y is carbon content (see Table 1). The water content is shown in Table 1 and plotted as a function of surface area in Figure 3. The initial total water content of the samples was constant for the experiments since the temperature and relative humidity (RH) are maintained at 22–25 °C and 43–53%, respectively, in our laboratory.

Calorimetry. High-temperature oxide melt solution calorimetry was performed in a home-built Tian-Calvet twin calorimeter operating at 973 K and using sodium molybdate, $3Na_2O{\cdot}4MoO_3$, as the solvent.[19,20] Pelletized samples (~5 mg) were dropped into a platinum crucible containing 20 g of melt. An oxidizing atmosphere was maintained in the calorimeter by flushing the headspace above the crucible with oxygen at 30 mL/min and by bubbling oxygen through the solvent at 5 mL/min.

The initial calorimetric data were corrected for carbon and hematite in the coarse-grained maghemite samples B-1 and B-2. Even though the carbon content in the samples was low, the heat effect of carbon oxidation to gaseous CO_2 at 973 K is large (−383.3 kJ/mol) (Table 2), so the correction is significant. The correction was done as follows:

$$\Delta H_{ds} = \Delta H_{ds} + \Delta H_{ds(C)}y \quad (3)$$

where ΔH_{ds} is high-temperature drop solution enthalpy, $\Delta H_{ds(C)}$ is enthalpy of drop solution of carbon, −383.3 kJ/mol (heat of carbon oxidation plus heat content of CO_2; see Table 2), and y is carbon content in moles (Table 1).

Although the calorimetry was done on all the samples listed in Table 1, we only accepted the data of the samples in which the carbon content did not exceed 1.5 wt %. Values for the drop solution of coarse-grained maghemite samples B-1 and B-2 were corrected for the presence of hematite using the calorimetric cycle depicted in Table 3.

As a cross-check, the enthalpy of solution for several samples was also measured in a Hart Scientific IMC-4400 isothermal calorimeter as was described in detail in previous works.[22,23] The experiments were done at 298 K and used a standardized solution of 5.00 N HCl (Alfa Aesar) as the solvent. The experimental data are plotted together with previously obtained acid solution calorimetric data[12] for maghemite that was synthesized by a wet synthesis method. Since these new data only cover high surface areas, they were fitted together with previous[12] data for maghemite with low surface area. Because of the low solubility of carbon in HCl, there is a negligible contribution to the total heat effect and the calorimetric data were not corrected for the carbon. This is a big advantage compared to the high-temperature calorimetric data, where carbon oxidation contributes almost 400 kJ per mole of carbon or about.

Water adsorption calorimetry at 25 °C was carried out in an apparatus which interfaces a Micromeritics ASAP 2000 gas adsorption analyzer with a Setaram DSC111 Calvet microcalorimeter as described in detail elsewhere.[21–24] Prior to the adsorption experiment, several tests were performed to determine the optimum degas conditions for both samples. The highest temperature at which bulk samples (C-1) can be degassed without being reduced to magnetite is 250 °C. For the fine-grained sample (Ah-1) this temperature is 150 °C. Thus, the bulk sample (C-1) was degassed at 250 °C for at least 12 h, and the fine-grained sample (Ah-1) was degassed at 150 °C for at least 12 h. After the initial, high-temperature degassing, both samples were degassed for 48 h at 25 °C. The amount of water remaining after the final degassing is critical for the correction of the high temperature calorimetric data. Thus, the amount of remaining water was determined from the weight loss of the sample upon firing the degassed samples at 1100 °C in air as described for the furnace experiments. The degassed samples were weighed in an argon filled glovebox to prevent water pickup. The amount of remaining water was 0.03 ± 0.01 mol of H_2O per Fe_2O_3 for the bulk sample C-1 and 0.16 ± 0.01 mol of H_2O per Fe_2O_3 for the fine-gained sample Ah-1.

Results and Discussion

A very important issue was proving that maghemite samples had no magnetite admixture (either in solid solution

(19) Navrotsky, A. *Phys. Chem. Miner.* **1977**, *2*, 89.
(20) Navrotsky, A. *Phys. Chem. Miner.* **1997**, *24*, 222.
(21) Ushakov, S. V.; Navrotsky, A. *Appl. Phys. Lett.* **2005**, *87*, 164103/1.
(22) Majzlan, J.; Mazeina, L.; Navrotsky, A. *Geochim. Cosmochim. Acta* **2007**, *71*, 615.
(23) Mazeina, L.; Deore, S.; Navrotsky, A. *Chem. Mater.* **2006**, *18*, 1830.
(24) Mazeina, L.; Navrotsky, A. *Chem. Mater.* **2007**, *19*, 825.

Table 2. Thermodynamic Cycle for Calculation of Heat Effect of Oxidation of Carbon Admixture in Fe_2O_3 to CO_2 at 973 K[a]

reaction	reference data
$C_{xl,298K} + O_{2g,973K} = CO_2\uparrow_{g,973K}$	$\Delta H_1 = \Delta H_{ds}(C)$
$CO_{2g,298K} = CO_{2g,973K}$	ΔH_2 = heat content of CO_2 from 298 to 973 K = 31.9 kJ/mol[26]
$C_{xl,298K} + O_{2g,298K} = CO_{2g,298K}$	$\Delta H_3 = \Delta H^0_f(CO_2) = -393.5$ kJ/mol[26]
$O_{2g,298K} = O_{2g,973K}$	ΔH_4 = heat content of O_2 from 298 to 973 K = 21.7 kJ/mol[26]
$\Delta H_{ds}(C) = \Delta H_1 = \Delta H_2 + \Delta H_3 - \Delta H_4 = -383.3$ kJ/mol	

[a] ΔH_{ds} = drop solution enthalpy.

Table 3. Thermodynamic Cycle and Reference Calorimetric Data for Calculation of Enthalpy of Formation ΔH_f of Nano-Maghemite from High-Temperature Calorimetry at 973 K in $3Na_2O \cdot 4MoO_3$ and from Acid Solution Calorimetry at 298 K[a]

reaction	reference data
High-Temperature Calorimetry	
γ-$Fe_2O_{3xl} \cdot xH_2O_{l,298K} = Fe_2O_{3sln,973K} + xH_2O\uparrow_{g,973K}$	$\Delta H_1 = \Delta H_{ds}(\gamma\text{-}Fe_2O_3) \cdot xH_2O$
α-$Fe_2O_{3,298K} = Fe_2O_{3sln,973K}$	$\Delta H_2 = \Delta H_{ds}(\alpha\text{-}Fe_2O_3) = 93.7 \pm 0.9$ kJ/mol
$Fe_{xl,298K} + 1.5O_{2g,298K} = \alpha\text{-}Fe_2O_{3xl,298K}$	$\Delta H_3 = \Delta H^0_f(\alpha\text{-}Fe_2O_3) = -826.2 \pm 1.3$ kJ/mol[26]
$H_2O_{l,298K} = H_2O_{g,973K}$	$\Delta H_4 = 68.9$ kJ/mol[26]
$Fe_{xl,298K} + 1.5O_{2g,298K} = \gamma\text{-}Fe_2O_{3xl,298K}$	$\Delta H_5 = \Delta H^0_f(\gamma\text{-}Fe_2O_3)$
Correction of ΔH_{ds} of Maghemite Containing 8 wt % of 20 nm Hematite	
$\Delta H_5 = \Delta H^0_f(\gamma\text{-}Fe_3O_3) = -\Delta H_1 + \Delta H_2 + \Delta H_3 + x\Delta H_4$	
$(\gamma\text{-}Fe_2O_3 \cdot xH_2O_{L,298K})_{0.92}(\alpha\text{-}Fe_2O_3 \cdot yH_2O_{l,298K})_{0.08} = Fe_2O_{3sln,973K} + (0.92x + 0.08y)H_2O_{g,973K}$	$\Delta H_{ds} = \Delta H_{ds}(\text{nano-}\gamma\text{-}Fe_2O_3 \cdot xH_2O)_{0.92}(\text{nano-}\alpha\text{-}Fe_2O_3 \cdot yH_2O)_{0.08}$
$\text{nano-}\alpha\text{-}Fe_2O_3 \cdot yH_2O_{L,298K} = Fe_2O_{3sln,973K} + yH_2O_{g,973K}$	$\Delta H_7 = \Delta H_{ds}(\text{nano-}\alpha\text{-}Fe_2O_3 \cdot yH_2O) = 92.9 \pm 2.7$ kJ/mol
ΔH_{ds} corr $= (\Delta H_{ds} + 0.08\Delta H_7)/0.92$	
Acid Solution Calorimetry	
$\gamma\text{-}Fe_2O_{3xl} \cdot xH_2O_l + [6H^+]_{aq} = [2Fe^{3+} + (3 + x)H_2O]_{aq}$	$\Delta H_1 = \Delta H_{sol}(\gamma\text{-}Fe_2O_{3xl} \cdot xH_2O)$
$\gamma\text{-}FeOOH_{xl} + [3H^+]_{aq} = [Fe^{3+} + (2 + w)H_2O]_{aq}$	$\Delta H_2 = \Delta H_{sol}(\gamma\text{-}FeOOH \cdot wH_2O) = -46.5 \pm 0.2$[28]
$H_2O_l = H_2O_{aq}$	$\Delta H_3 = \Delta H_{dilution} = -0.5$[27]
$H_{2g} + {}^1/_2O_{2g} = H_2O_l$	$\Delta H_4 = \Delta H^0_f(H_2O) = -285.8 \pm 0.1$[26]
$Fe_{xl} + O_{2g} + {}^1/_2H_{2g} = \gamma\text{-}FeOOH_{xl}$	$\Delta H_5 = \Delta H^0_f(\gamma\text{-}FeOOH) = -549.4 \pm 1.4$[11]
$Fe_{xl} + 1.5O_{2g} = \gamma\text{-}Fe_2O_{3xl}$	$\Delta H_6 = \Delta H^0_f(\gamma\text{-}Fe_2O_3)$
$\Delta H_5 = \Delta H^0_f(\gamma\text{-}Fe_2O_3) = -\Delta H_1 + 2\Delta H_2 + (1 - x)\Delta H_3 + \Delta H_4 + 2\Delta H_5$	

[a] g = gas, l = liquid, xl = crystal, sln = solution, aq = aqueous species.

with maghemite or as a separate phase). In other words, one needed to make sure all iron was ferric. Since maghemite and magnetite have similar patterns and since distinguishing between these two phases is very difficult with the broad XRD, Mossbauer, and FTIR peaks, some magnetite admixtures cannot be completely excluded only on the basis of these analyses. Nevertheless, TGA analysis showed no weight gain. Thus, the maximum concentration of magnetite in nanomaghemite is about 1 wt %.

The temperature of the maghemite → hematite phase transformation depends on many factors,[17] including adsorbed species and particle size. This transformation is irreversible as the particles coarsen. We observed that for smaller particles (2–10 nm) the temperature of this transformation in air was 783–823 K, whereas for larger particles (30–43 nm, samples B1 and B2) it was 753–763 K. These last samples also had a minimum amount of carbon that might contribute to the temperature shift as well since the transition temperature depends on adsorbed species as well.[17] Enthalpy of transformation of sample Ah-8 (fine-grained maghemite to hematite of unknown grain size) calculated from the DSC curve (shown in Figure 2) is −25 kJ/mol.

Complete weight loss of the samples occurred by ∼673 K. Carbon content in this sample was less than 1 wt %; thus, we assume that water is responsible for almost all of the weight loss. Since this is relatively low temperature for the removal of all water, we conclude that the water adsorbed on maghemite is mostly physically bound. For comparison, to remove all the water on hematite, one needs to heat it to 973–1073 K.[24] This is additional evidence that surface water adsorbed on maghemite is bonded less strongly than on hematite.

Nanomaghemite contains up to 1 mol of water per Fe_2O_3 (Figure 3). Since samples were synthesized in the absence of aqueous solvents, all the water must be adsorbed by the surface after the synthesis (during the storage or handling of the samples in air).

Water adsorption experiments were performed on two samples (C-1 and Ah-1) and showed reasonably consistent results. Adsorption isotherms are shown in Figure 4a. Calorimetric results are shown in Figure 4b as a function of surface coverage θ in H_2O molecules/nm^2. The coverage was calculated after the quantity of adsorbed water was corrected for adsorption on the sample holder walls. This correction was less than 1% for the fine-grained sample but was 15% for the bulk sample, which explains the larger experimental error for the latter. A summary of the water adsorption experiments is given in Table 4.

The heat effect corresponding to the adsorption of one dose is the differential enthalpy of adsorption.[22,24] All the water adsorbed with a differential enthalpy more negative than −44 kJ/mol will be called chemically adsorbed or strongly bound water, and water adsorbed with enthalpy at the liquid water level (−44 kJ/mol, equal to the heat of vapor condensation) will be called physically adsorbed water or weakly bound water. The reference state for the differential enthalpy of adsorption is vapor. Integral enthalpy relative to vapor is the sum of the differential enthalpies divided by the total amount of adsorbed water.[22,24] We use liquid water as a

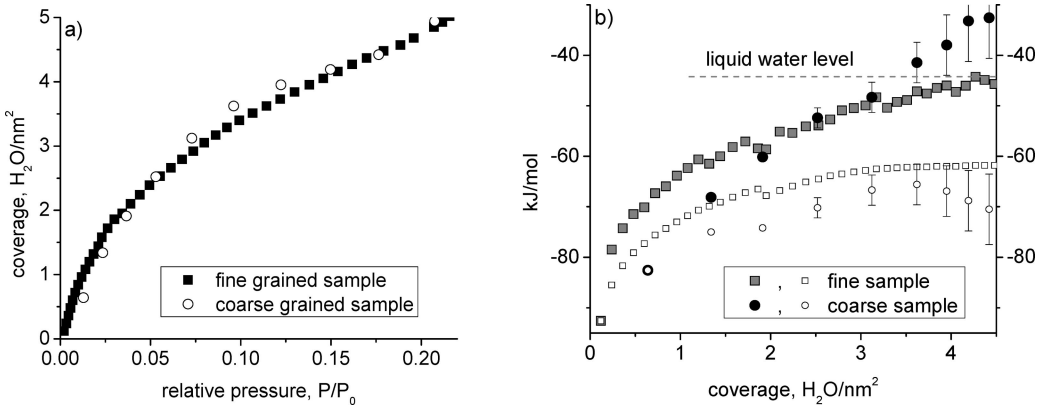

Figure 4. Results of water vapor adsorption experiments: (a) relative pressure; (b) differential (filled symbols) and integral (open symbols) enthalpies of water adsorption for fine-grained sample Ah-1 (squares) and for coarse-grained sample C-1 (circles).

Table 4. Results of Water Adsorption Calorimetry

		water remaining after degas			coverage at liquid water level H_2O/nm^2	
sample ID	initial water H_2O/nm^2	n mol/Fe_2O_3	H_2O/nm^2	integral ΔH_{ads}, kJ/mol, of H_2O per Fe_2O_3 at liquid water level[a]	H_2O/nm^2	% of total strongly bound water [b]
Ah-1	18.2 ± 0.9	0.16 ± 0.06	5.2 ± 1.9	−61.8 ± 1.8	4.5 (9.7 ± 1.9)[a]	59 ± 12
C-1	18.8 ± 1.6	0.03 ± 0.01	4.7 ± 1.6	−68 ± 10	4.5 (9.2 ± 1.6)[a]	49 ± 9
average:	18.4 ± 0.9		5.0	−65 ± 10	4.5 (9.5 ± 2.5)[a]	54 ± 16

[a] Relative to vapor. Integral enthalpies relative to liquid water are obtained by adding 44 kJ/mol to these values. [b] Remaining after degas water plus water corresponding to the coverage at liquid water level; ΔH_{ads} = enthalpy of adsorption.

Table 5. Acid Solution and Oxide Melt Solution Calorimetric Data[a]

		acid calorimetry		oxide melt solution calorimetry		
sample ID	surface area, $m^2/mol \times 10^3$	ΔH_{sln}, kJ/mol, of $Fe_2O_3 \cdot xH_2O$	ΔH_{sln} (ads. corr), kJ/mol, of Fe_2O_3	ΔH_{ds}, kJ/mol, of $Fe_2O_3 \cdot xH_2O \cdot yC$	ΔH_{ds}, H_2O and C corr	ΔH_{ds} (ads corr), kJ/mol, of Fe_2O_3
Ah-8	34.2	−116.0 ± 1.2	−119.7	31.1 ± 2.5	52.2	47.5
As-7	32.5			22.8 ± 1.0	66.4	62.6
As-6	30.0			51.9 ± 1.4	56.5	51.0
Ah-3	24.5	−118.2 ± 1.2	−120.5			
Ah-2	22.9	−107.6 ±3.1	−109.6	31.4 ± 1.3	79.2	75.7
Ah-1	20.2	−108.2 ± 3.3	−110.6	65.3 ± 1.9	68.5	65.5
B-2	8.8			74.5 ± 1.9	83.8	82.5
B-1	3.7			72.9 ± 1.7	76.4	75.8

[a] ΔH_{sln} = solution enthalpy, ΔH_{ds} = drop solution enthalpy.

reference state for the integral water adsorption enthalpies; therefore, 44 kJ/mol is added to all values of integral adsorption enthalpy relative to vapor. These values relative to the liquid are used in all further calculations and comparisons. The coverage at which the differential enthalpy of water adsorption reaches the energetics of liquid water and the integral enthalpies of water adsorption are in reasonable agreement for both samples (Figure 4, Table 4). We used integral enthalpies of water adsorption relative to liquid water to correct calorimetric data for the adsorbed water as follows:

$$\Delta H_{ds,sln}(corr) = \Delta H_{ds,sln} + \Delta H_{chem} c \qquad (4)$$

where $\Delta H'_{ds,sln}$ is high-temperature drop solution (corrected for carbon) or acid solution enthalpy, ΔH_{chem} is the integral enthalpy of adsorption for chemically bound water, −21.0 kJ/mol, and c reflects the stoichiometric coefficient for the chemically bound water, which is equal to 0.54. The water remaining after degas is included in this coefficient (see Table 4). Initial, carbon corrected, and water corrected water calorimetric are given in Table 5.

Two sets of calorimetric data were used to calculate surface enthalpy for hydrous and anhydrous maghemite surfaces. The first set is calorimetric data (both high-temperature oxide melt and acid solution) corrected for zero enthalpy (relative to liquid water) of water adsorption.[22–24] The slope of the linear fit of these data plotted versus surface area gives the surface enthalpy of hydrated maghemite. The second set of data is corrected for the adsorbed water using the measured enthalpy of water. The slope of the linear fit of the second data set plotted versus surface area gives the enthalpy of the anhydrous surface (Figure 5). The rationale for this methodology has been presented earlier.[22–24] For additional cross-checks and comparisons, the enthalpies of formation were calculated from the current acid solution data, from the previous data from acid calorimetry,[12] and from the high-temperature calorimetric data using cycles depicted in Table 3. The obtained enthalpies of formation are plotted as a function of surface area (Figure 6).

For both samples, the coverage at which the differential enthalpy of water adsorption equals the energetics of liquid water is $\theta \sim 4.5$ H_2O/nm^2 (Table 4). This coverage combined with the water remaining after degas corresponds to the strongly adsorbed water, which is ∼54% of all water

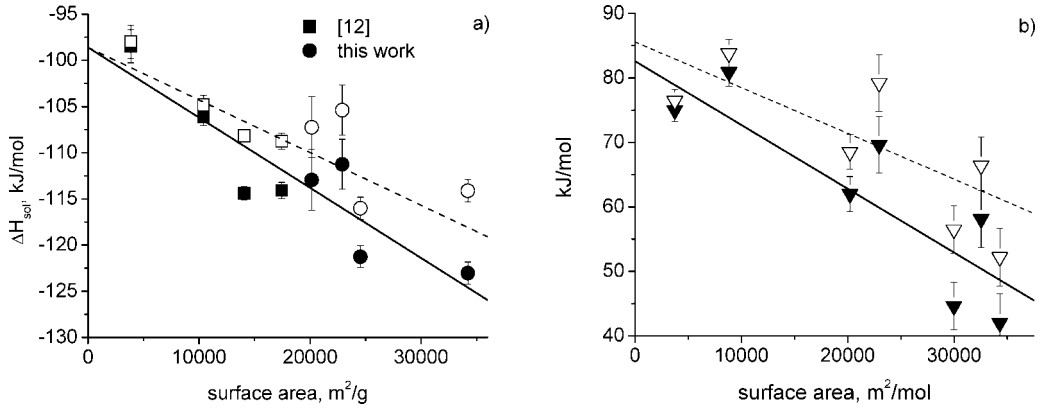

Figure 5. Acid solution (a) and high-temperature oxide melt solution (b) calorimetric data. Filled symbols represent data point corrected for strongly adsorbed water; linear fit of these data points (solid line) represents the surface enthalpy for anhydrous surface. Open symbols represent data points where no enthalpy of water adsorption was applied to correct for adsorbed water; linear fit of these data points (dashed line) represents the enthalpy of hydrated surface.

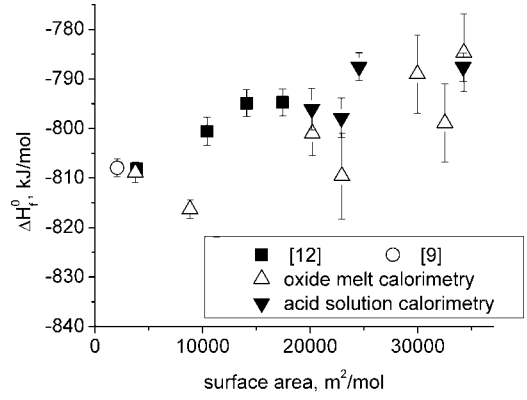

Figure 6. Enthalpies of formation from the elements at $T = 298$ K as a function of the surface area of nanomaghemite samples.

adsorbed (see Table 4). The integral enthalpy of water adsorption on maghemite, obtained in our work (0.50 ± 0.03 J/m^2), is in good agreement with the heat of immersion of maghemite degassed at 200 °C, obtained by Watanabe and Seto[25] (0.513 J/m^2). The average integral enthalpy of water adsorption at this coverage for the two samples is -21 ± 10 kJ/mol (Table 4). The average was used to correct acid solution and high temperature calorimetry data.

Slopes of the linear fit of the acid solution (Figure 5a) and the high-temperature oxide melt (Figure 5b) calorimetric data, corrected for the measured enthalpy of water adsorption, give the surface enthalpy of the anhydrous surface. The value from acid solution calorimetry (0.71 ± 0.13 J/m^2) and the value from high-temperature oxide melt calorimetry (0.99 ± 0.25 J/m^2) agree within experimental error. These are the first known reported values for enthalpy of the anhydrous surface of γ-Fe_2O_3.

In previous works,[22–24] we emphasized that, if one assumes that the adsorbed surface water has the energetics of liquid water, the slope of the calorimetric data versus surface area would be the surface enthalpy of the hydrated surface. The surface enthalpy of the hydrated maghemite surface in this work is 0.57 ± 0.10 J/m^2 from acid solution calorimetry and is 0.63 ± 0.28 J/m^2 from high-temperature oxide melt calorimetry. These values agree within experimental error and also agree with values reported by Majzlan[12] (0.83 ± 0.18 J/m^2) and Diakonov[7] (0.61 ± 0.11 J/m^2). The observed difference between surface enthalpy of hydrated and anhydrous surfaces is relatively small for an oxide but is typical for oxyhydroxides[22–24] that have more relaxed surfaces due to the structural OH groups. All values of surface enthalpy are shown in Table 6. The recommended values for the surface enthalpy of maghemite are the more accurate ones obtained using acid solution calorimetry.

Table 6. Surface Enthalpy ΔH_s of Maghemite Samples Calculated before and after Water Correction

hydrated surface, J/m^2	"dry" (water free) surface, this work, J/m^2
0.83 ± 0.18[12]	
0.61 ± 0.11[7,8]	
0.63 ± 0.28 (oxide melt solution calorimetry)	0.99 ± 0.25 (oxide melt solution calorimetry)
0.57 ± 0.10 (acid solution calorimetry)	0.71 ± 0.13 (acid solution calorimetry)

The previous value of standard enthalpy of formation of maghemite, -808.1 ± 2.0 kJ/mol,[11] was obtained for maghemite having 0.116 mol of water and surface area 18 m^2/g. The value of the standard enthalpy of formation for anhydrous maghemite with zero surface area, calculated using the above values for surface enthalpy and enthalpy of water adsorption, is -811.5 ± 2.2 kJ/mol.

As seen from Figure 5, the calorimetric data for maghemite scatter for both calorimetric methods. Less scatter was observed for other iron oxides.[12,22–24] This scatter can be partially explained by the sensitivity of the data to carbon and water corrections. Another factor may be the complexity of maghemite structure, especially at the nanoscale. Unfortunately, the broad diffraction peaks make analysis of lattice defects, superstructure formation, and detection of solid solution with magnetite or magnetite admixtures[17] difficult. The energetics of maghemite may also depend on the method of synthesis, the precursor used, and/or the particle shape.[29]

(25) Watanabe, H.; Seto, J. *Bull. Chem. Soc. Jpn.* **1988**, *61*, 3067.
(26) Robie, R. A.; Hemingway, B. S.; Fisher, J. R. Thermodynamic properties of minerals and related substances at 298.15 K and 1 bar (10^5 Pascals) pressure and at higher temperature. U.S. Geol. Survey Bull., 1995.
(27) Parker, V. B. Thermal properties of uni-univalent electrolytes. National Standard Reference Data Series, National Bureau of Standards, 1965.
(28) Majzlan, J.; Navrotsky, A.; Schwertmann, U. *Geochim. Cosmochim. Acta* **2004**, *68*, 1049.

Table 7. Comparison of Physical−Chemical Data of Hematite and Maghemite

	hematite, α-Fe_2O_3	maghemite, γ-Fe_2O_3
standard enthalpy of formation, kJ/mol	−826.2 ± 1.3	−811.6 ± 2.2
standard free energy of formation, kJ/mol	−744.3 ± 1.3	−731.0 ± 2.2[a]
enthalpy of liquid water adsorption, kJ/mol	−67 ± 4.9[24]	−21 ± 10
strongly adsorbed water, H_2O/nm^2	11–13[24]	9.5
point of zero charge[25]	6.8	5.4
surface site density, sites/nm^2 [31]	4.55 ± 0.25	0.81 ± 0.05
surface enthalpy:		
hydrated surface, J/m^2	0.75 ± 0.16[12]	0.57 ± 0.10
anhydrous surface, J/m^2	1.9 ± 0.3[24]	0.66 ± 0.13

[a] Calculated using enthalpy from this work and entropy from Majzlan et al.[10]

All these factors could affect the calorimetric data and could cause the larger scatter. Nevertheless, the data obtained offer a reasonable constraint on surface enthalpy.

Comparison of Maghemite with Hematite. There are only a few published studies on the thermodynamics of maghemite surface properties, but there are many studies of hematite surface properties. In general, our study agrees with ideas in the literature that the enthalpy of water adsorption on hematite is more exothermic than that on maghemite.[25] Surfaces with larger surface enthalpies, such as those of hematite, bind water more strongly than those with smaller surface enthalpies, such as those of maghemite. The concentration of chemically adsorbed water on maghemite, 9.5 H_2O/nm^2, is somewhat less than that on hematite (13 H_2O/nm^2).[24] It was reported[31] that under the same experimental conditions (pH, ionic strength) hematite exhibits a considerably higher surface site density, 4.55 ± 0.25 sites/nm^2, compared to 0.81 ± 0.05 sites/nm^2 for maghemite. Although other values of the surface density of hematite have been reported as well,[32] the numbers from Jarlbring et al.[31] probably give a reasonable ratio between the active sites of maghemite and hematite because they were obtained under the same experimental conditions. The total water (all adsorbed water including physically adsorbed water) on maghemite is less than that on hematite (Figure 3), perhaps due to greater distances between neighboring hydroxyl groups on the maghemite surfaces than on the hematite surfaces.[25] The polarization of the bonds in bulk hematite is stronger than for bulk maghemite. This effect extends to the surface groups,[25] resulting in stronger attraction between the hematite surface and the adsorbed species than that for maghemite. A summary of physical−chemical properties of hematite and maghemite is given in Table 7 for comparison.

The difference in the surface energetics of hematite and maghemite is consistent with several well-established trends. First, the thermodynamically less stable (in the bulk) phase (maghemite) has a smaller surface enthalpy than the more stable one (hematite), and the most stable phase shows a more exothermic heat of water adsorption. Second, the polymorph with a higher value of point of zero charge has a larger heat of water adsorption compared to one with smaller PZC.[25,30]

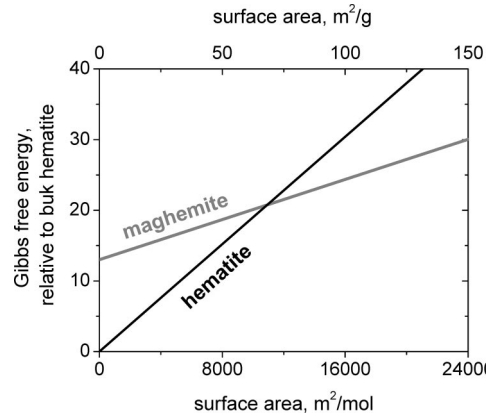

Figure 7. Energy crossover between hematite and maghemite as function of "water-free" surface area.

Differences in enthalpies as a function of surface area create crossovers in enthalpy and probably free energy (stability) as well. Figure 7 shows the energy crossover between hematite and maghemite assuming no water had been adsorbed on the surface; i.e., the surfaces are "dry". Although for coarse samples maghemite is metastable relative to hematite by ∼15 kJ/mol in enthalpy and by ∼13 kJ/mol in Gibbs free energy,[10,11,26] maghemite becomes stable at surface area of ∼70–80 m^2/g. This corresponds to a particle size of ∼15 nm. Conversely, hematite is more stable than maghemite at low surface areas. A temperature-driven phase transition from maghemite (seen in DSC) suggests that the hematite formed is coarser than the initial maghemite. The observed heat release during the TG/DSC run (−25 kJ/mol, see Figure 2) was more exothermic than that of transition between bulk maghemite and bulk hematite (−15 kJ/mol), but less exothermic than that of fine-grained maghemite → bulk hematite (about −35 kJ/mol). Thus, even though the transformation of fine-grained maghemite does not lead to a very coarse hematite, it is still strongly exothermic, and probably, an intermediate size hematite forms. A direct size-driven phase transition between hematite and maghemite was observed with milling[33] which also supports our findings of size-related stabilities of hematite and maghemite. A similar energy crossover was observed for the Al_2O_3 system where the difference between surface enthalpies of α- and γ-polymorphs is similar to that for the Fe_2O_3 system.[34,35]

Conclusions

Energetics of fully characterized maghemite nanoparticles with surface areas up to ∼200 m^2/g and particle size 2–40 nm was investigated by high-temperature oxide melt and acid solution calorimetry. Approximately 54% of the total water is strongly adsorbed with an average enthalpy of adsorption of −21 kJ/mol relative to liquid water and –65 kJ/mol relative to vapor. The rest of the water is weakly bound with an enthalpy of adsorption of −44 kJ/mol relative to vapor, which is equal to the enthalpy of water condensation. The surface

(29) Chopra, G. S.; Real, C.; Alcala, M. D.; Perez-Maqueda, L. A.; Subrt, J.; Criado, J. M. *Chem. Mater.* **1999**, *11*, 1128.

(30) Watanabe, H.; Seto, J.; Nishiyama, Y. *Bull. Chem. Soc. Jpn.* **1993**, *66*, 2751.

enthalpy obtained from acid solution calorimetry is 0.57 ± 0.10 J/m^2 for the hydrated surface and 0.71 ± 0.13 J/m^2 for the anhydrous surface. The small values of surface enthalpy, the small value of water adsorption enthalpy relative to liquid water, and the relatively small amount of strongly adsorbed water agree with the literature observations of lower site density and weaker polarization of bonds in maghemite compared to hematite.

The difference in the surface enthalpy for the dry surface between α- and γ-polymorphs of Fe_2O_3 is similar to that between α- and γ-Al_2O_3. This large difference (~1.2 J/m^2) creates energy crossovers so that fine-grained hematite is metastable relative to fine-grained maghemite at a particle size of ~15 nm or less. Maghemite stability at high surface areas makes it possible to synthesize ultrafine maghemite nanoparticles.

Acknowledgment. Financial support from DOE Grant DEFG03-97ER14749 is gratefully acknowledged. We thank S. Ushakov for help with water adsorption experiments. We thank J. Majzlan for giving us the opportunity to use his samples and data for cross-checks of our calorimetric data. John Neil is thanked for useful discussions.

CM071178O

(31) Jarlbring, M.; Gunneriusson, L.; Hussmann, B.; Forsling, W. *J. Colloid Interface Sci.* **2005**, *285*, 212.
(32) Cromieres, L.; Moulin, V.; Fourest, B.; Giffaut, E. *Colloids Surf., A* **2002**, *202*, 101.
(33) Randrianantoandro, N.; Mercier, A. M.; Hervieu, M.; Greneche, J. M. *Mater. Lett.* **2001**, *47*, 150.
(34) McHale, J. M.; Auroux, A.; Perrota, A. J.; Navrotsky, A. *Science* **1997**, *277*, 791.
(35) McHale, J. M.; Navrotsky, A.; Perrotta, A. J. *J. Phys. Chem. B* **1997**, *101*, 603.